DOI 10.1007/s10946-024-10222-5
Journal of Russian Laser Research, Volume 45, Number 3, May, 2024

NANOCRYSTALLINE DIAMOND FILMS GROWN IN CH_4-H_2-GeH_4-N_2 GAS MIXTURES: STRUCTURE AND LUMINESCENT CHARACTERISTICS

Artem Martyanov,[1] Ivan Tiazhelov,[1] Sergey Savin,[1,2] and Vadim Sedov[1*]

[1] *Prokhorov General Physics Institute, Russian Academy of Sciences*
Vavilov str. 38, Moscow, 119991, Russia

[2] *MIREA – Russian Technological University*
Vernadsky Ave. 78, Moscow 119454, Russia

[*] Corresponding author e-mail: sedovvadim@yandex.ru

Abstract

The chemical vapor deposition (CVD) of diamond allows the controllable formation of the material with desirable structure and elemental composition. In this study, Ge-doped microcrystalline and nanocrystalline diamond (NCD) films are synthesized using microwave plasma-assisted CVD in CH_4-H_2-GeH_4-N_2 gas mixtures. We grow series of 2 μm thick NCD films with variations in gas composition $[N_2] = 0 - 4\%$ and $[CH_4] = 10 - 15\%$. We investigate and compare the structure, phase composition, and luminescent characteristics of the grown films. The luminescent signals from Silicon vacancy (SiV, 738 nm) and Germanium vacancy (GeV, 602 nm) color centers in diamond are registered. The additional annealing of the as-grown films in air is used to remove the excessive sp^2 phase that hinders their luminescent properties. For both SiV and GeV centers, we find conditions for CVD growth of NCD films that are as bright or even brighter than Si-doped and Ge-doped high-quality microcrystalline diamond films (MCD) grown without N_2 additions. These results may be used for the fabrication of NCD films and plates with high concentrations of SiV and GeV centers, which may serve as source material for the fabrication of sub-micrometer-sized luminescent diamond particles for local optical thermometry.

Keywords: polycrystalline diamond, chemical vapor deposition, color centers, Germanium vacancy.

1. Introduction

Luminescent diamond materials attract significant attention due to their possible applications in quantum-information technologies (single-photon sources), biomedicine (optical biomarkers), and local optical thermometry [1]. Such materials may be produced by chemical vapor deposition (CVD) in the forms of single crystals [2,3], polycrystalline films [4,5], membranes [6,7], and separate particles [8–10].

The CVD method allows doping of the grown diamond with various impurities, which may form color centers in normally-transparent diamond, such as Nitrogen-vacancy (NV) [11], Silicon-vacancy (SiV) [12–14], Germanium-vacancy (GeV) [15], Tin-vacancy (SnV) [16,17], etc. These centers are now widely used in photonics and biomedicine [18]. Recently, Savvin et al. demonstrated that diamond with NV centers might be used as an active laser medium [19].

Specifically, the GeV color center in diamond possesses a narrow-band photoluminescence (PL) emission in the orange spectral range (602 nm) [20–24]. This color center can be formed during the CVD synthesis of diamond with either a gaseous or a solid-state source of Ge atoms in the reactor.

Manuscript submitted by the authors in English on April 23, 2024.

In recent work, Romshin et al. [9] showed a great perspective of using diamond particles with such color centers as local optical thermometers. For that goal, sub-micrometer-sized diamond particles with a strong PL signal should be fabricated. One of the ways to produce large quantities of such small particles is to grow polycrystalline diamond (PCD) films with an average grain size close to the required size of particles, with the aim of consecutive milling the film obtained [25, 26]. In our previous work [27], we demonstrated that such Ge-doped nano-crystalline diamond (NCD) films might be grown, using gaseous monogermane (GeH_4) or solid-state Ge plates as a dopant source. However, in this study, the use of N_2 gas addition to stimulate the formation of NCD films; see, e.g., [28, 29] where the disappearance of the SiV and GeV peaks in the PL spectra of the films was demonstrated without notable degradation of the film structure.

Our aim in this work is to investigate the mechanisms of the formation of GeV centers in diamond during its synthesis with the CVD technique in CH_4-H_2-GeH_4 and CH_4-H_2-GeH_4-N_2 gas mixtures. We systematically vary the composition of gas mixtures in a microwave plasma CVD (MPCVD) reactor to grow the Ge-doped diamond and investigate how it affects the structure and luminescent characteristics of NCD films. Additional annealing of the grown films in air is used to remove the sp^2 phase formed during CVD. For the first time, we demonstrate the dynamics of decrease of the PL intensity of SiV and GeV centers in MPCVD-grown NCD diamond films with increase in the N_2 concentration in CH_4-H_2-GeH_4-N_2 gas mixtures.

2. Experimental

As the initial substrates, we use polished single-crystal (100) Silicon wafers with dimensions of $10\times10\times0.35$ mm^3. Substrates are seeded using a suspension of nano-diamond particles (particle sizes of 3–7 nm, Zeta potential > +50 mV, Cardiff University [30–32]) by spin coating the wafers at 3000 rpm. Ge and N-doped polycrystalline diamond films are grown, employing MPCVD reactor ARDIS-100 (2.45 GHz, Optosystems Ltd, Russia) [33, 34] in methane-hydrogen-monogermane-nitrogen (CH_4-H_2-GeH_4-N_2) gas mixtures with a fixed total gas flow at 500 sccm. The film thickness is directly controlled during synthesis by a laser interferometer [33], and the final thickness of all PCD films is 2 μm for all samples. The total deposition time varies between 40 and 115 min. for different samples. Substrate temperatures are measured with the two-color pyrometer (METIS M322, SensorTherm GmbH, Steinbach, Germany). CVD conditions, like a substrate temperature of $850\pm15^\circ$ C, a pressure of 53 Torr, a microwave power of 3.5 kW, and a monogermane-to-methane concentration of $[GeH_4]/[CH_4] = 1.5\%$ are fixed for all samples. We choose these conditions based on our previous works [**?**, 35, 36] to obtain the high-intensity GeV PL signal and minimize the formation of the cubic Germanium as a separate phase [35, 36]. Polycrystalline diamond films are grown at various nitrogen-to-total-gas flow concentrations ν_N from 0 to 4%. For each ν_N four samples, two are grown at the methane-to-total-gas flow concentration $\nu_c = 10\%$ and two, at $\nu_c = 15\%$. The surface morphology of the samples and crystal sizes are examined, using Tescan MIRA3 scanning electron microscope (SEM), equipped with an energy-dispersive X-ray spectroscopy (EDX) module for elemental analysis. Raman and PL spectra at room temperature are taken with LabRam HR840 (Horiba) spectrometer in a confocal configuration. The laser beam of 473 nm wavelength is focused on an ≈ 1 μm spot on the sample surface (Olympus BX41). We record the Raman spectra on each sample from three random points. The variance of values between different points does not exceed 5%; therefore, below, the average values of the intensities are shown.

3. Results and Discussion

3.1. SEM Characterization

Scanning electron microscope (SEM) is utilized to examine the morphology of the synthesized diamond films. In Fig. 1, we show the SEM images of the surface of the MPCVD-grown Ge and N-doped polycrystalline diamond films at methane-to-total-flow concentration $[CH_4] = 10\%$ and $[CH_4] = 15\%$ and different nitrogen-to-total-flow concentration $[N_2]$. Without nitrogen addition and $[CH_4] = 10\%$, diamond films have a microcrystalline (MCD) structure with an average grain size of 2 μm. But at $[CH_4] = 15\%$, under the same conditions, an intermediate state between microcrystalline and nanocrystalline structures of diamond film is formed, which has an agglomerate structure with a crystallite size of up to 100 nm. In our previous work [37], it was shown that a higher methane concentration (at a substrate temperature above 800°C) stimulated secondary nucleation processes and facilitated the formation of the NCD structure of PCD films. As we see in Fig. 1, even a small nitrogen addition (0.4%) accelerates sharply this process to form NCD films.

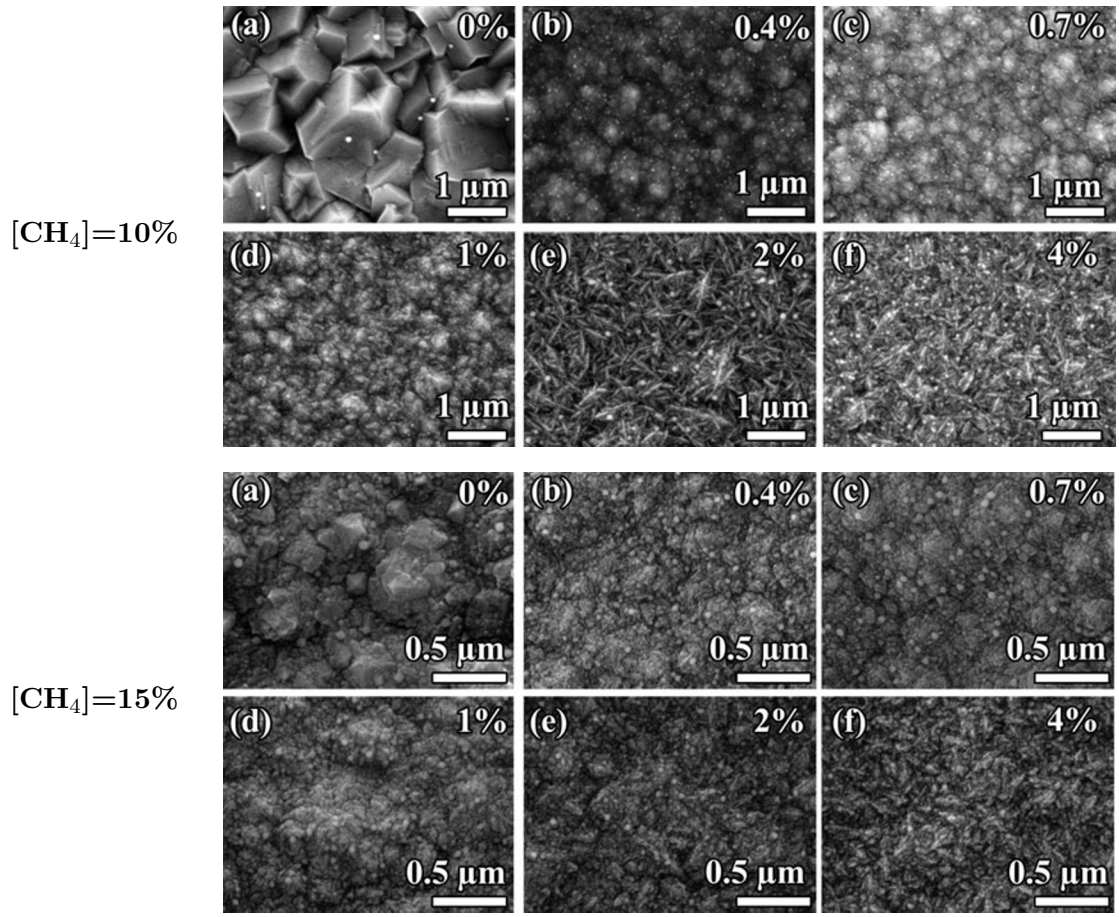

Fig. 1. SEM images of polycrystalline Ge-doped and N-doped diamond films synthesized at CH_4 to total flow concentration $[CH_4] = 10\%$ and $[CH_4] = 15\%$ and different N_2 to total flow concentration $[N_2]$.

3.2. Raman Spectroscopy

We use Raman spectroscopy for a comprehensive analysis of the structural quality of the diamond films. To remove the sp^2 phase of carbon, the samples are annealed in air in a laboratory-made electric furnace at temperatures of $\approx 590^\circ$ C for 5 h. In Fig. 2, we show Raman spectra of polycrystalline Ge-diamond films synthesized at CH_4 to total flow concentration $[CH_4] = 10\%$ and $[CH_4] = 15\%$ and different N_2 to total flow concentration $[N_2]$ before (a, c) and after (b, d) air annealing.

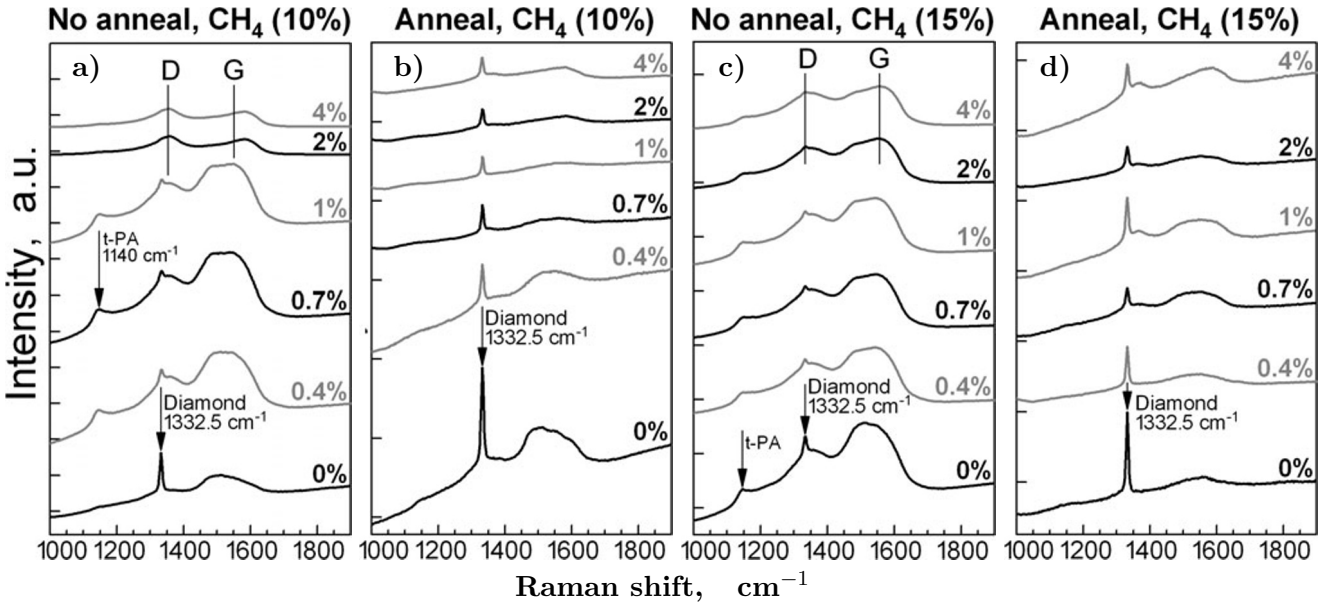

Fig. 2. Raman spectra of Ge-doped and N-doped diamond films synthesized at CH_4 to total flow concentration $[CH_4] = 10\%$ (a, b) and $[CH_4] = 15\%$ (c, d) and different N_2 to total flow concentration $[N_2]$ before (a, c) and after (b, d) air annealing. Here, t-PA (1140 cm^{-1}), diamond (1332.5 cm^{-1}), D (1350 cm^{-1}), and G (1550 cm^{-1}) peaks are shown.

Raman spectrum at $[CH_4] = 10\%$ and $[N_2] = 0\%$ is typical for MCD film and contains the narrow unshifted diamond peak at 1332.5 cm^{-1}. At higher N_2 concentrations, a peak of t-PA is at 1140 cm^{-1}, while D and G peaks at 1350 and 1550 cm^{-1}, respectively, appear, being belong to the sp^2 phase of carbon; they are common for NCD films. Increase in the $[N_2]$ concentration results in increase in the intensities of sp^2 peaks in comparison with sp^3 one, which should be taken into account when analyzing PL spectra. In Fig. 2, one can see that the air annealing leads to a significant reduction in the intensity of all sp^2-related peaks in spectra with respect to the sp^3 (diamond) peak at 1332.5 cm^{-1}.

3.3. PL Spectroscopy

To investigate the optical properties of the films, we use photoluminescence (PL) spectroscopy; the spectra are shown in Fig. 3. In these spectra, the main features of the films are GeV (602 nm) and Silicon-vacancy (SiV, 738 nm) peaks, which serve as an evidence of the incorporation of Ge and Si atoms, respectively, into the diamond grains. The source of Si atoms is contamination on the walls of the CVD reactor, which contains Si atoms due to the use of Si substrates in previous experiments; see, e.g., [27,38]. In all spectra, the SiV peak is much more intense than the GeV peak; this is explained by the difficulties

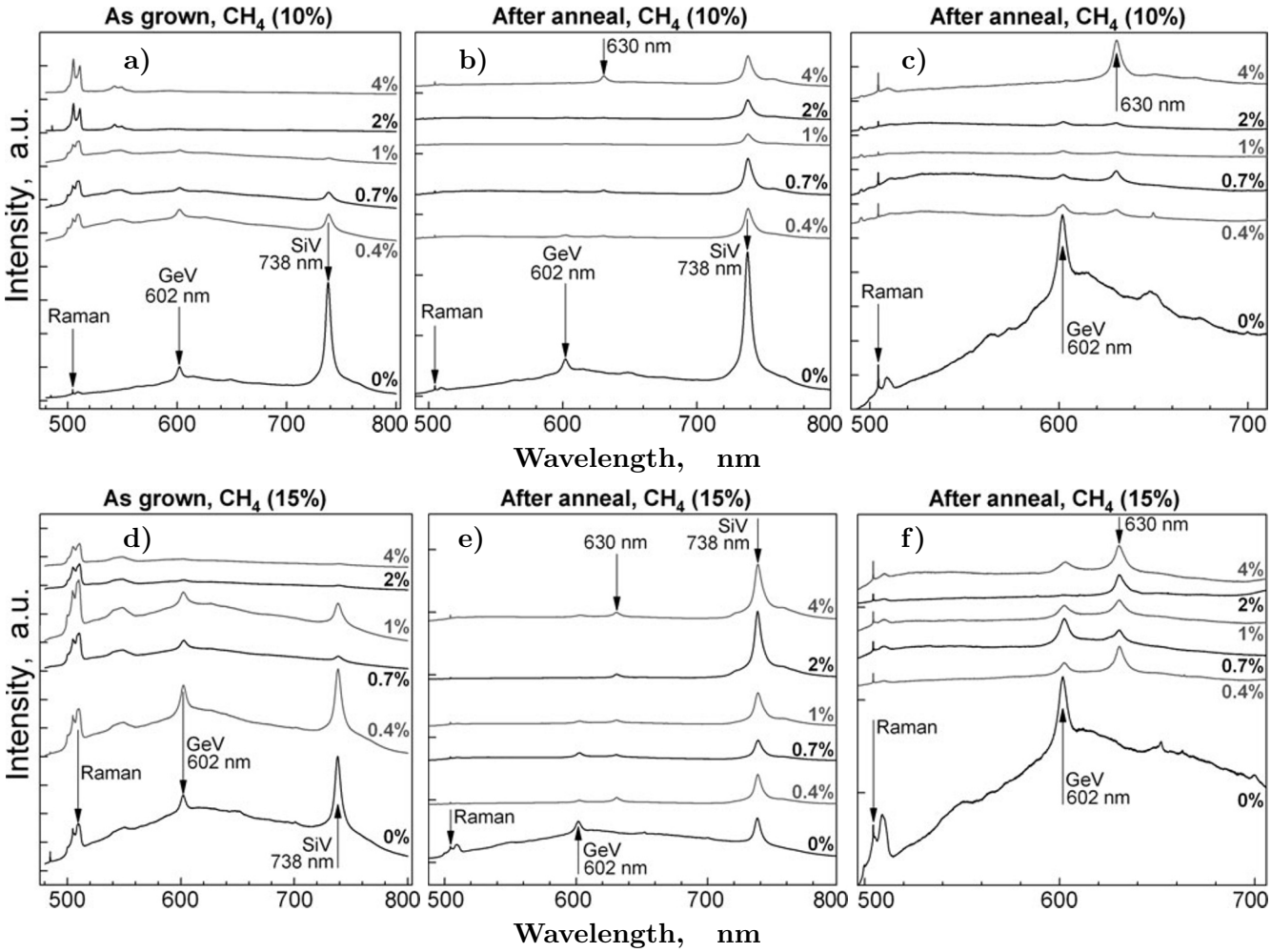

Fig. 3. PL spectra of Ge-doped and N-doped diamond films CVD-grown in CH_4-H_2-GeH_4-N_2 gas mixtures at various $[N_2]$ concentrations; here, $[CH_4] = 10\%$ before (a) and after (b, c) air annealing and $[CH_4] = 15\%$ before (d) and after (e, f) air annealing. Also, (c) and (f) are shown close-ups of (b) and (e), respectively, for a better visibility of the GeV peak at 602 nm.

of incorporation of large atoms into the dense diamond lattice; it was discussed in detail in [17, 39]. No signal from NV^0 (575 nm) or NV^- (637 nm) color centers is observed.

Similarly to our previous work [27], at nitrogen concentrations $[N_2] = 4\%$, there are no notable SiV and GeV peaks in PL spectra. However, at concentrations of $[N_2] \leq 1\%$, both SiV and GeV peaks reappear, yet far from being as intense as for MCD films ($0\%N_2$). The interesting finding is, that in cases of high nitrogen concentrations $[N_2] = 2 - 4\%$, the air annealing allows the observation of a SiV peak that is not notable in the spectra of the as-grown material. The addition of small amounts of nitrogen also improves the PL intensity of GeV centers (before annealing). Thus, the formation of SiV and GeV centers is not stopped by the addition of N_2. However, the formation of additional sp^2 that is caused by N_2 additions [40] can sufficiently hinder the luminescence of color centers. The annealing selectively etches away the sp^2 phase, which allows the registration of SiV centers again. However, the effect of air annealing on PL intensity of GeV centers is in its reduction rather than the expected increase. NCD

films are known to be vulnerable to the annealing in air at 600°C [41], so defective diamond can also be etched. With that, GeV defects seem to be etched rather actively, while SiV defects are more resistant to such air annealing and benefit from it. This observation may be explained by Ge being a larger atom than Si, so GeV defects distort dense crystal lattice of diamond more than SiV defects, and they are first to be etched under harsh air annealing conditions.

In addition to GeV and SiV, at high N_2 and CH_4 concentrations, the 630 nm peak also can be noticed after annealing. This peak is often observed in CVD-grown polycrystalline films, however, its exact nature is still unknown [42].

For a proper comparison, all PL intensities are normalized to the diamond Raman peak at 1332.5 cm^{-1} (505 nm in PL spectra). The normalized dependence plots of "SiV-to-Diamond" and "GeV-to-Diamond" on $[N_2]$ before and after annealing are shown in Fig. 4. It is expected that the PL intensity of SiV and GeV color centers in a high-quality MCD film ($[CH_4] = 10\%$, $[N_2] = 0\%$) would be superior to any NCD film. However, for both SiV and GeV, there are CVD conditions that allowed obtaining similar or even higher PL signal in NCD films, e.g., $[CH_4] = 10\%$, $[N_2] = 4\%$ with air annealing for SiV, and $[CH_4] = 15\%$, $[N_2] = 0.7\%$ without air annealing for GeV. The positive role of high methane concentrations on the intensity of GeV centers was also noticed in our previous work [27]. However, in the case of the GeV center, we note that annealing reduces the "GeV-to-Diamond" ratio rather than increasing it. We assume

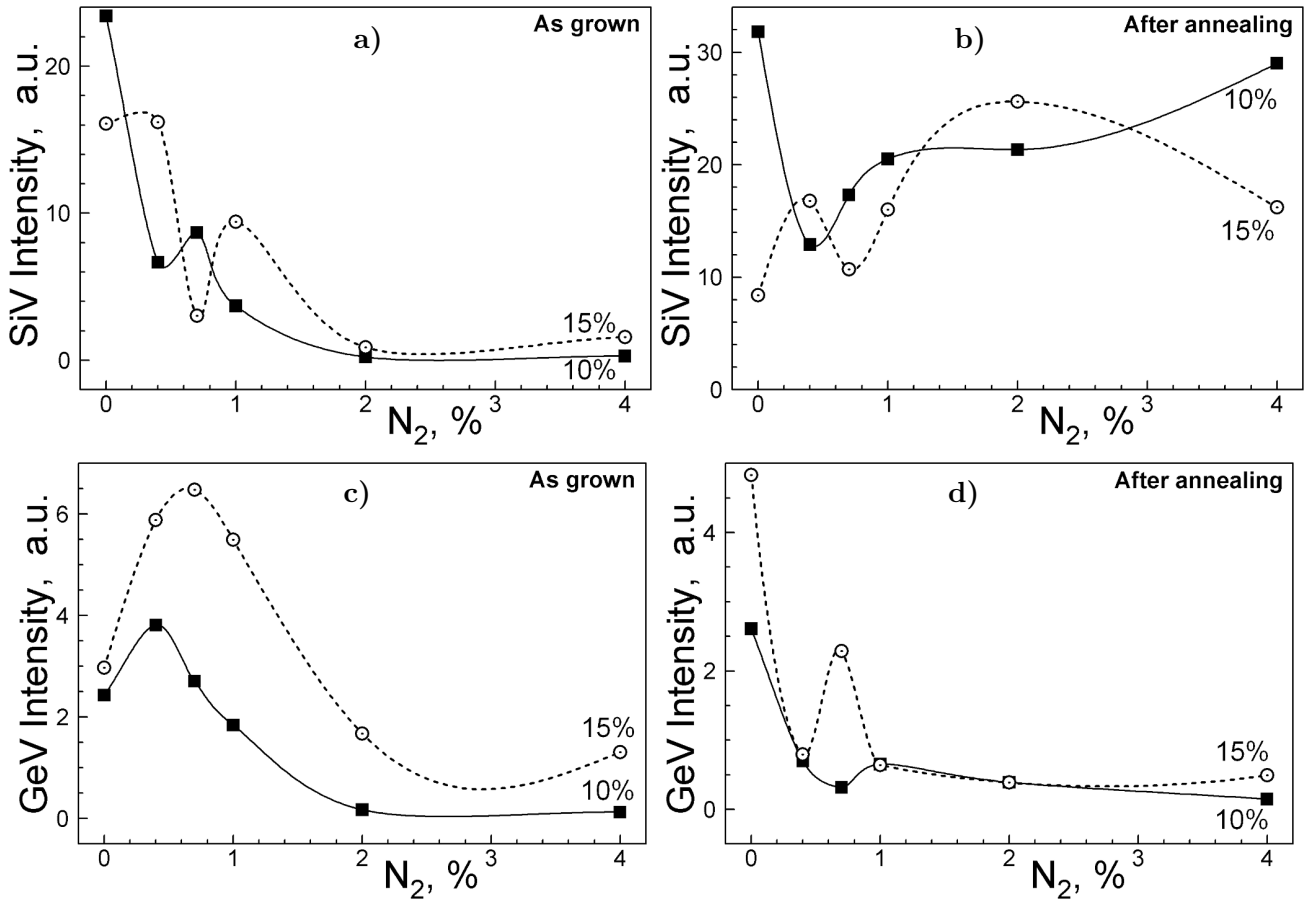

Fig. 4. SiV-to-Diamond (a, b) and GeV-to-Diamond (c, d) ratios before (a, c) and after (b, d) air annealing.

that this drop in intensity may be avoided by a proper choice of milder annealing conditions specifically for GeV centers. However, such investigation lies beyond the current work and is left for further study.

4. Summary

We studied the synthesis of NCD films by MPCVD in CH_4-H_2-GeH_4-N_2 gas mixtures. The results obtained showed that the use of nitrogen additions during the growth did not prevent the formation of NCD films with intense SiV and GeV signals. However, in the as-grown material, the excessive sp^2 phase could hinder its luminescent properties. The annealing in air allowed removing the sp^2 phase to significantly increase the PL signal from SiV centers in diamond grains.

The attained results may be used for the fabrication of polycrystalline diamond films and plates with high concentrations of SiV and GeV centers, which may serve as a starting material for the fabrication of sub-micrometer-sized luminescent diamond particles for local optical thermometry.

Acknowledgments

The work was funded by the Russian Science Foundation under Grant No. 21-72-10153; see `rscf.ru/project/21-72-10153/`. The authors would like to thank Dr. Soumen Mandal (Cardiff University, UK) for the provision of aqueous suspensions of nanodiamonds.

References

1. N. Nunn, A. I. Shames, M. Torelli, et al., in *Lumin. Nanomater.*, Jenny Stanford Publishing (2022), pp. 1–95.
2. M. A. Lobaev, A. M. Gorbachev, S. A. Bogdanov, et al., *Diam. Relat. Mater.*, **72**, 1 (2017).
3. A. Tallaire, O. Brinza, P. Huillery, et al., *Carbon*, **170**, 421 (2020).
4. V. Sedov, V. Ralchenko, A. Khomich, et al., *Diam. Relat. Mater.*, **56**, 23 (2015).
5. B. Yu, B. Yang, H. Li, et al., *Appl. Surf. Sci.*, **552**, 149475 (2021).
6. V. S. Sedov, A. A. Voronin, M. S. Komlenok, et al., *J. Russ. Laser Res.*, **41**, 321 (2020); DOI: 10.1007/s10946-020-09881-x
7. A. Yu. Klokov, A. I. Sharkov, V. G. Ralchenko, V. S. Sedov, *J. Russ. Laser Res.*, **42**, 580 (2021); DOI: 10.1007/s10946-021-09996-9
8. M. T. Westerhausen, A. T. Trycz, C. Stewart, et al., *ACS Appl. Mater. Interfaces*, **12**, 29700 (2020).
9. A. M. Romshin, V. Zeeb, A. K. Martyanov, et al., *Sci. Rep.*, **11**, 14228 (2021).
10. S. A. Grudinkin, N. A. Feoktistov, K. V. Bogdanov, et al., *Phys. Solid State*, **62**, 919 (2020).
11. R. Schirhagl, K. Chang, M. Loretz, and C. L. Degen, *Annu. Rev. Phys. Chem.*, **65**, 83 (2014); DOI: 10.1146/annurev-physchem-040513-103659
12. I. I. Vlasov, A. A. Shiryaev, T. Rendler, et al., *Nat. Nanotechnol.*, **9**, 54 (2014).
13. V. Ralchenko, V. Sedov, V. Saraykin, et al., *Appl. Phys. A*, **122**, 795 (2016).
14. M. M. Quarshie, S. Malykhin, and P. Kuzhir, *Opt. Mater. Express*, **14**, 965 (2024).
15. V. Sedov, A. Martyanov, I. Tiazhelov, et al., *Diam. Relat. Mater.*, **138**, 110206 (2023).
16. T. Iwasaki, *Semicond. Semimet.*, **103**, Elsevier (2020), pp. 237–256; DOI: 10.1016/bs.semsem.2020.03.007
17. V. Sedov, A. Martyanov, A. Neliubov, et al., *Philos. Trans. R. Soc. Math. Phys. Eng. Sci.*, **382**, 20230167 (2024); DOI: 10.1098/rsta.2023.0167
18. I. Aharonovich and E. Neu, *Adv. Opt. Mater.*, **2**, 911 (2014).
19. A. Savvin, A. Dormidonov, E. Smetanina, et al., *Nat. Commun.*, **12**, 1 (2021).
20. V. G. Ralchenko, V. S. Sedov, A. A. Khomich, et al., *Bull. Lebedev Phys. Inst.*, **42**, 165 (2015).

21. E. A. Ekimov, S. G. Lyapin, K. N. Boldyrev, et al., *JETP Lett.*, **102**, 701 (2015).
22. T. Iwasaki, F. Ishibashi, Y. Miyamoto, et al., *Sci. Rep.*, **5**, 12882 (2015).
23. A. Komarovskikh, V. Nadolinny, V. Plyusnin, et al., *Diam. Relat. Mater.*, **79**, 145 (2017).
24. M. Nahra, D. Alshamaa, R. Deturche, et al., *AVS Quantum Sci.*, **3**, 012001 (2021).
25. S. Heyer, W. Janssen, S. Turner, et al., *ACS Nano*, **8**, 5757 (2014).
26. T. Asano, Y. Oobuchi, and S. Katsumata, *J. Vac. Sci. Technol. B*, **13**, 431 (1995); DOI: 10.1116/1.587963
27. V. S. Sedov, A. K. Martyanov, A. S. Altakhov, et al., *J. Russ. Laser Res.*, **43**, 503 (2022); DOI: 10.1007/s10946-022-10076-9
28. V. Podgursky, A. Bogatov, V. Sedov, et al., *Diam. Relat. Mater.*, **58**, 172 (2015).
29. V. Podgursky, A. Bogatov, M. Yashin, et al., *Diam. Relat. Mater.*, **92**, 159 (2019).
30. S. Mandal, *RSC Adv.*, **11**, 10159 (2021).
31. H. A. Bland, I. A. Centeleghe, S. Mandal, et al., *ACS Appl. Nano Mater.*, **4**, 3252 (2021).
32. V. Sedov, A. Martyanov, E. Ashkinazi, et al., *Surf. Interfaces*, **38**, 102861 (2023); DOI: 10.1016/j.surfin.2023.102861
33. V. Sedov, A. Martyanov, A. Altakhov, et al., *Coatings*, **10**, 939 (2020).
34. V. S. Sedov, A. K. Martyanov, A. A. Khomich, et al., *Diam. Relat. Mater.*, **109**, 108072 (2020).
35. V. Sedov, A. Martyanov, S. Savin, et al., *Diam. Relat. Mater.*, **90**, 47 (2018).
36. V. Ralchenko, V. Sedov, A. Martyanov, et al., *Carbon*, **190**, 10 (2022).
37. A. Martyanov, I. Tiazhelov, S. Savin, et al., *Coatings*, **13**, 751 (2023).
38. V. S. Sedov, I. I. Vlasov, V. G. Ralchenko, et al., *Bull. Lebedev Phys. Inst.*, **38**, 291 (2011).
39. E. A. Ekimov, S. G. Lyapin, and M. V. Kondrin, *Diam. Relat. Mater.*, **87**, 223 (2018).
40. V. Sedov, A. Martyanov, S. Savin, et al., *Diam. Relat. Mater.*, **114**, 108333 (2021); DOI: 10.1016/j.diamond.2021.108333
41. A. Martyanov, I. Tiazhelov, S. Savin, et al., *Coatings*, **13**, 751 (2023).
42. K. Bray, R. Sandstrom, C. Elbadawi, et al., *ACS Appl. Mater. Interfaces*, **8**, 7590 (2016).